

The origin of the eccentricity of the hot Jupiter in CI Tau

G. P. Rosotti,¹★ R. A. Booth,¹ C. J. Clarke,¹ J. Teyssandier,² S. Facchini³
and A. J. Mustill⁴

¹*Institute of Astronomy, University of Cambridge, Madingley Road, Cambridge CB3 0HA, UK*

²*Department of Applied Mathematics and Theoretical Physics, University of Cambridge, Wilberforce Road, Cambridge CB3 0WA, UK*

³*Max-Planck-Institut für Extraterrestrische Physik, Giessenbachstrasse 1, D-85748 Garching, Germany*

⁴*Lund Observatory, Department of Astronomy and Theoretical Physics, Lund University, Box 43, SE-221 00 Lund, Sweden*

Accepted 2016 September 13. Received 2016 September 9; in original form 2016 June 27

ABSTRACT

Following the recent discovery of the first radial velocity planet in a star still possessing a protoplanetary disc (CI Tau), we examine the origin of the planet’s eccentricity ($e \sim 0.3$). We show through long time-scale (10^5 orbits) simulations that the planetary eccentricity can be pumped by the disc, even when its local surface density is well below the threshold previously derived from short time-scale integrations. We show that the disc may be able to excite the planet’s orbital eccentricity in <1 Myr for the system parameters of CI Tau. We also perform two-planet scattering experiments and show that alternatively the observed planet may plausibly have acquired its eccentricity through dynamical scattering of a migrating lower mass planet, which has either been ejected from the system or swallowed by the central star. In the latter case the present location and eccentricity of the observed planet can be recovered if it was previously stalled within the disc’s magnetospheric cavity.

Key words: accretion, accretion discs – planets and satellites: dynamical evolution and stability – planet–disc interactions – protoplanetary discs – stars: pre-main-sequence.

1 INTRODUCTION

The recent discovery of a radial velocity planet in the young, disc bearing star CI Tau (Johns-Krull et al. 2016) offers the first opportunity to test theories for the formation and early evolution of hot Jupiters in discs. To date, planet discoveries in discs have derived from direct imaging (e.g. Chauvin et al. 2004, 2005; Neuhäuser et al. 2005, 2008; Marois et al. 2008; Kraus & Ireland 2012; Sallum et al. 2015) due to difficulties in applying transit detection and radial velocity methods in young stars. The presence of discs evidently rules out transit detections (though candidate transit detections have been obtained in disc-less young stars: van Eyken et al. 2012; Ciardi et al. 2015; David et al. 2016). Both the transit and radial velocity techniques are impeded by the extreme variability of young stars (Xiao et al. 2012; Stauffer et al. 2014); in particular it is difficult to disentangle companion induced radial velocity variations from the quasi-periodic signals produced by star-spots. In the case of CI Tau, however, this effect has been minimized using *K* band (where star-spot activity is reduced); this has allowed the extraction of a radial velocity periodicity (9 d) distinct from the photometric period (7 d, plausibly ascribed to stellar rotation).

The planet parameters in CI Tau ($P = 9$ d, $M_{\text{sin}i} = 8.1 M_{\text{Jup}}$) place it firmly in the ‘hot Jupiter’ category. In contrast to another

hot Jupiter recently found around a T Tauri star (Donati et al. 2016), CI Tau also possesses a massive circumstellar disc of $\sim 37 M_{\text{Jup}}$ as deduced from previous mm observations using Plateau de Bure interferometer (Guilloteau et al. 2011; see also Andrews & Williams 2007); if the inclination inferred from the outer disc (45° to 54° ; Guilloteau et al. 2014) is also the inclination of the planet then the measured $M_{\text{sin}i}$ corresponds to a mass of $\sim 10 M_{\text{Jup}}$.

Given the impossibility of forming giant planets *in situ* in close proximity to the host star,¹ there is a long-standing debate about the origin of hot Jupiters: whether they arrive in their present locations during the gas-rich phase (by disc mediated migration and/or scattering of planetary embryos) or whether instead by dynamical scattering after the disc has dispersed (Lin, Bodenheimer & Richardson 1996; Rasio & Ford 1996). The recent discovery in CI Tau provides a key demonstration that in at least one object the former is the case.

The relatively high eccentricity ($e = 0.3 \pm 0.16$)² is however somewhat unexpected in a scenario of purely disc mediated migration, as discs tend to damp planetary eccentricity (Papaloizou &

¹ See Chiang & Laughlin (2013) and Hansen & Murray (2013) for *in situ* formation models for planets considerably less massive than that in CI Tau.

² See fig. 5 of Johns-Krull et al. (2016) for a plot of the distribution of the possible values.

* E-mail: rosotti@ast.cam.ac.uk

Larwood 2000; Tanaka & Ward 2004).³ Although the eccentricity of massive planets can be excited by the disc (Papaloizou, Nelson & Masset 2001; D’Angelo, Lubow & Bate 2006; Bitsch et al. 2013), Dunhill, Alexander & Armitage (2013) have argued that this requires that the disc surface density in the vicinity of the planet falls in a restricted range: we will revisit this conclusion through long time-scale FARGO3D integrations of disc–planet systems in Section 2. Alternatively, such eccentricities can be driven by interactions involving multiple planets (Marzari, Baruteau & Scholl 2010; Moeckel & Armitage 2012; Lega, Morbidelli & Nesvorný 2013); in the case of CI Tau, the absence of another period in the radial velocity data implies that any perturbing giant planet is no longer in the sub-au region and in Section 3 we explore, through two-planet FARGO3D simulations and through simply parametrized scattering experiments, whether there are orbital histories that can generate significant eccentricity in the observed planet while also removing the perturber from the inner disc.

We emphasize that this paper is mainly concerned with the excitation of eccentricity in the CI Tau radial velocity planet and we do not present an exhaustive set of scenarios for the system’s prior evolutionary history. In Section 4, we discuss whether the planet is likely to have acquired its eccentricity at its current position and whether its present location – close to but not at the radius of corotation between the disc and the star – is significant.

2 DISC-DRIVEN ECCENTRICITY GROWTH

Papaloizou et al. (2001) first showed that disc-driven eccentricity growth (long established in the case of stellar binaries: e.g. Lubow 1991a,b) can be extended to the regime of massive planets, attributing this growth to an instability launched at the 3:1 outer Lindblad resonance which excites disc eccentricity. More generally, for gap opening planets, Goldreich & Tremaine (1980) showed that Lindblad resonances lead to growth of eccentricity while corotation resonances lead to its damping (see also Goldreich & Sari 2003; Teyssandier & Ogilvie 2016). D’Angelo et al. (2006) argued for growth of eccentricity for Jupiter mass planets, because of contributions from several Lindblad resonances that lie near the disc edges (like the 2:4 and 3:5 resonances, with the 1:3 resonance being unimportant here), while corotation resonances are saturated and cannot damp eccentricity (see also Duffell & Chiang 2015).

The planet in CI Tau is thus in the regime where previous authors have found that the disc drives eccentricity; this finding extends to the 3D smoothed particle hydrodynamics (SPH) study of Dunhill et al. (2013) who also proposed a further criterion for eccentricity driving in terms of a minimum disc surface density in the vicinity of the planet, Σ . This can be expressed via a dimensionless parameter $q_{\text{disc}} = \pi \Sigma a^2 / M_p$, where a and M_p are the planet orbital radius and mass. Dunhill et al. (2013) proposed that eccentricity driving requires $q_{\text{disc}} > 0.075$; for lower disc surface densities, the eccentricity rises modestly over a few hundred orbits but then declines again.

In CI Tau, the value of q_{disc} can be estimated from the observed accretion rate on to the star ($\dot{M} = 3 \times 10^{-8} M_{\odot} \text{ yr}^{-1}$, McClure et al. 2013) and the disc temperature at ~ 0.1 au derived from spectral energy distribution modelling (~ 1700 K, Andrews & Williams 2007): in a steady state $\dot{M} = 3\pi\nu\Sigma$ where ν is the kinematic viscosity. Adopting the conventional α parametrization for disc viscosity

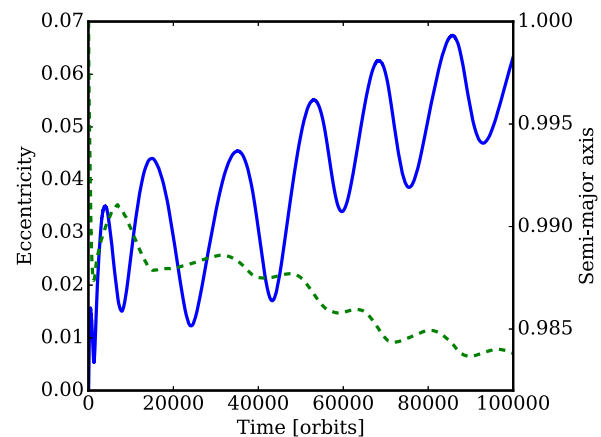


Figure 1. Eccentricity (solid blue) and semimajor axis (dashed green) of the planet as a function of time from the FARGO3D simulation of a single planet in a disc with $q_{\text{disc}} = 0.015$.

(Shakura & Sunyaev 1973) with $\alpha = 10^{-3}$ [towards the lower end of the range of values found in simulations of the magnetorotational instability in the inner disc (e.g. Suzuki, Muto & Inutsuka 2010; Flock et al. 2013)], we obtain an upper limit $q_{\text{disc}} < 0.014$.⁴

Our upper limit on the value of q_{disc} is at face value below the threshold required for eccentricity driving proposed by Dunhill et al. (2013). However, they were only able to pursue their computationally expensive 3D SPH simulations over a relatively short time interval (a few hundred orbits). Given that their simulations show fair agreement with the 2D grid based simulations of Papaloizou et al. (2001), it is of interest to use the FARGO3D code (Benítez-Llambay et al. 2016) in 2D, exploiting graphic processing units which accelerate the code significantly, in order to pursue long time-scale integration of the disc/planet system.

Previous works have either used a ‘live’ approach where the planet orbital parameters are free to evolve, or fixed them and derived their instantaneous rate of change by post-processing. Here, we choose the former approach, which we motivate later. The simulation is locally isothermal and we assume that the disc aspect ratio varies as $0.036(R/a)^{0.215}$ (Andrews & Williams 2007). We also adopt $\alpha = 10^{-3}$ at the location of the planet and a surface density power-law exponent of 0.3 (as derived from sub-mm imaging), scaling α with radius as $\alpha \propto R^{-0.63}$ in order to create a steady state profile in the absence of the planet. The numerical grid extends from 0.2 to 15 in dimensionless units; the surface density is exponentially tapered, with a tapering radius of 5, to prevent artefacts developing at the outer boundary (since these were found to affect the results in early tests). The resolution is 430 cells, logarithmically spaced, in radius and 580 in azimuth. The planet has a mass ratio to the central star of 0.013 and is initially fixed on a circular orbit at radius 1 for the first 50 orbits, during this period its mass gradually increases to its final value; thereafter its orbital parameters evolve freely. The disc surface density normalization implies $q_{\text{disc}} = 0.015$, similar to the upper limit derived above.

We evolve the system over 10^5 orbits (Fig. 1). On time-scales of hundreds of orbits, the eccentricity evolution is broadly similar to that seen in comparable models in Dunhill et al. (2013); differences (around a factor 3 in peak eccentricity attained) can be readily

³ Note that stellar tides raised in the planet are ineffective in modifying the eccentricity of a planet with these orbital parameters on an Myr time-scale (Barker & Ogilvie 2009).

⁴ Note that this value is more than three orders of magnitude higher than would be obtained by simply extrapolating the disc surface density profile inferred from sub-mm imaging on a scale of ~ 0.5 arcsec, i.e. ~ 70 au (Andrews & Williams 2007; Guilloteau et al. 2011).

ascribed to planet mass, disc density profile and viscosity. In both cases, the eccentricity declines from this first maximum.

However, our long-term simulations demonstrate that after $\sim 10^4$ orbits, the eccentricity begins to grow again and thereafter undergoes oscillatory behaviour superposed on a slow growth over the duration of the experiment. The oscillatory behaviour can be understood in terms of secular interaction between the planet and the disc: the disc develops an eccentric mode which cyclically exchanges eccentricity with the planetary orbit in a manner reminiscent of the secular interaction between two eccentric planets (Murray & Dermott 2000, chapter 7). A detailed analysis of this interaction is postponed to a future paper (Ragusa et al., in preparation). Note that this oscillatory interchange of eccentricity between the planet and the disc can only be captured by a ‘live’ (freely evolving planet) approach as adopted here. Oscillations appear also in the semimajor axis evolution, which further highlights the need for long-term integrations for studying migration of eccentric planets.

The final eccentricity is already in a regime that overlaps the broad range of eccentricity values admitted by current orbital solutions of the planet in CI Tau. More importantly, it is still rising at the end of the simulation; we estimate that at the current growth rate it will take 5×10^5 – 10^6 orbits to reach the best-fitting value of 0.3, which, given the short orbital time-scale at 0.1 au, is a small fraction of its current age (~ 1 Myr). The growth rate we measure is slightly lower, but roughly consistent with what was found by Teysandier & Ogilvie (2016) for similar local disc masses in the vicinity of the planet (see their fig. 14, although the different setups do not allow for a proper comparison).

We therefore conclude that our long time-scale integrations provide some preliminary evidence that the observed eccentricity of the planet in CI Tau may be the result of pumping by the disc.

3 ECCENTRICITY DRIVING BY A SIBLING PLANET

We now consider the alternative scenario in which the eccentricity of the observed planet is driven by dynamical interaction with another planet. Since we cannot explore the parameter space of multiple planet interactions with long-term hydrodynamical simulations we adopt the following approach. We first conducted a single FARGO3D simulation involving two planets and disc. We then compared the results with simple N -body simulations in which the effect of the disc is crudely modelled by applying damping of eccentricity and semimajor axis of either or both planets on prescribed time-scales, τ_e and τ_a (the latter is fixed to 7×10^5 yr).⁵ This comparison allowed us to calibrate the N -body simulations fixing the τ_e/τ_a ratio, which we then used in N -body calculations with a variety of planetary configurations.

Our hydrodynamical simulations used a similar setup to that described in Section 2, but we initially place a $3 M_{\text{Jup}}$ planet at $R = 1$ with a $10 M_{\text{Jup}}$ planet placed outside it in the 2:1 resonance. We adopt $q_{\text{disc}} = 0.01$ (normalizing to the mass of the larger planet) and model the radial domain up to $R = 8$. We allow the planets to migrate freely under the influence of the disc and follow their eccentricity evolution for $\sim 10^5$ orbits (Fig. 2). Within 10^4 orbits the

⁵ As discussed in Section 2, the disc is expected to drive a slow growth of eccentricity for single planets with masses above a few M_{Jup} . However, in resonant multiplanet systems, eccentricity is driven by planet–planet interactions and the disc’s role is to maintain the two planets close to resonance and to damp the eccentricity raised by this mutual interaction.

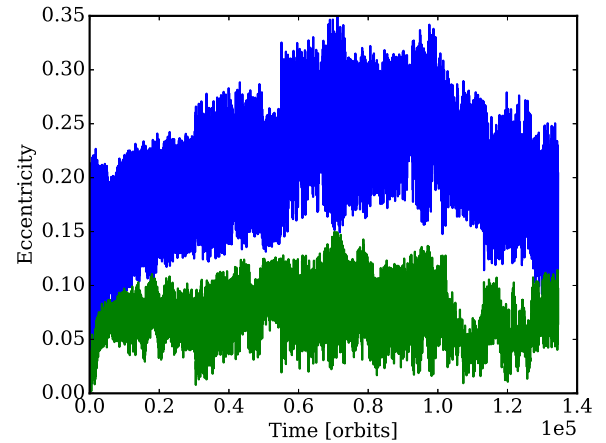


Figure 2. Eccentricity evolution of a $10 M_{\text{Jup}}$ planet (green) along with an interior $3 M_{\text{Jup}}$ planet (blue) in a two-planet FARGO3D simulation; time is in orbits at $R = 1$. See Section 3 for simulation parameters.

planets quickly reach moderate eccentricities, which remain steady (modulo some fluctuations) for the full 10^5 orbits.

The N -body calculations are performed using the code MERCURY (Chambers 1999), using the Burlisch–Stoer algorithm. Following Lee & Peale (2002) and Teysandier & Terquem (2014), we include additional damping forces in the N -body model to generate migration and eccentricity damping, and vary the ratio of eccentricity damping to migration time-scales (τ_e is actually half of the migration time-scale, Teysandier & Terquem 2014), τ_e/τ_a , to match the hydrodynamical simulation. The planets (with masses 3 and $10 M_{\text{Jup}}$, as in the hydro model) are initially given small eccentricities ($\sim 10^{-3}$) and inclinations ($\sim 0:01$). We consider two scenarios, either applying damping to both planets or only to the outer planet. Neglecting the damping of the inner planet may be a good description in the case of massive planets which open a deep gap in the disc and where the inner disc is expected to be depleted.

A comparison of Fig. 2 with Fig. 3 shows that the N -body models can be a fair match to simulations. When damping on both planets is included a value of τ_e/τ_a in the range 0.1–1 is needed, while when the inner planet is undamped we favour values in the range 0.01–0.1. We take $\tau_e/\tau_a = 0.1$ as a compromise. We note that our estimate of τ_e/τ_a exceeds the typical value of 0.01 estimated from analytical and numerical simulations of single planets with $M \lesssim 1 M_{\text{Jup}}$ (Papaloizou & Larwood 2000; Cresswell et al. 2007). This should not be surprising since we consider planets massive enough to open a deep gap, which means that the co-rotation torques responsible for damping the eccentricity are much weaker (which enables the disc-driven eccentricity growth considered in Section 2). The eccentricities attained at the end of the calculations shown in Fig. 3 are in broad agreement with the analytical results of Teysandier & Terquem (2014).

We now turn to the question of whether resonant eccentricity driving can generate $e \gtrsim 0.2$ as in the observed planet in CI Tau while simultaneously removing the sibling planet from a region where it would have been detected in the radial velocity data. To do this, we conducted a suite of N -body models. We initially place one planet at 0.1 au and migrate a second planet into resonance with it (after which they migrate in resonance together), following the subsequent eccentricity growth (which can lead to close scattering). In each case, we assume that one planet (which may be either the inner or outer planet) has mass $10 M_{\text{Jup}}$ and vary the mass of the sibling planet. The only sense in which these calculations are not

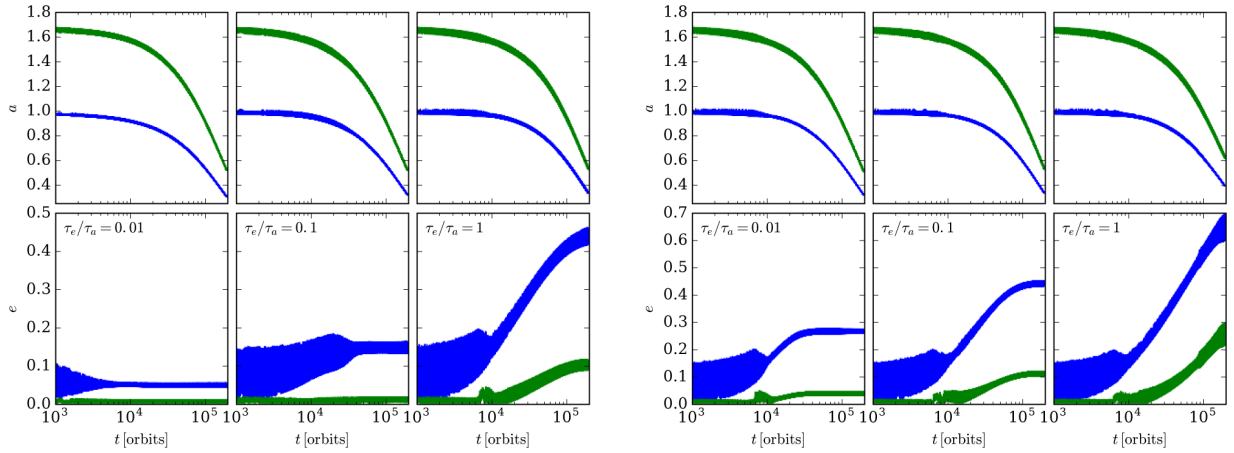


Figure 3. Evolution of eccentricity and semimajor axis in two-planet N -body calculations for different ratios of τ_e/τ_a (see text). A $3 M_{\text{Jup}}$ (blue) and a $10 M_{\text{Jup}}$ (green) are initially placed at dimensionless radii 1 and 1.66. Left-hand panel: eccentricity damping applied to both planets; right-hand panel: damping only of outer planet. Time is measured in orbits at the initial radius of the inner planet.

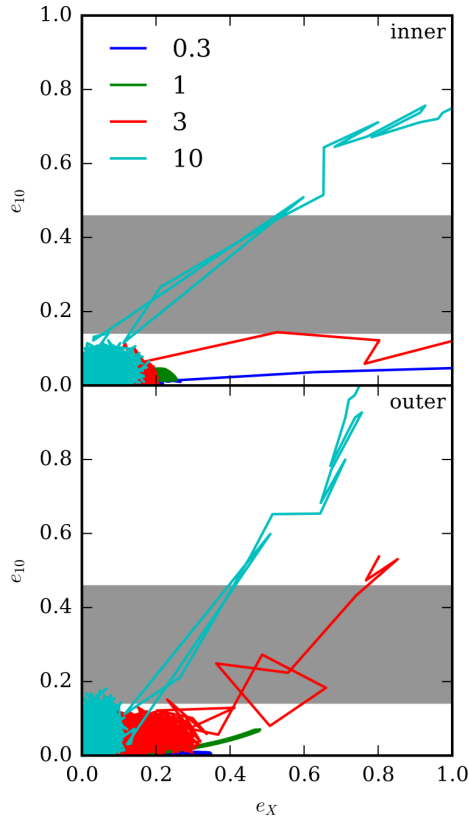


Figure 4. Eccentricity of the $10 M_{\text{Jup}}$ planet against the eccentricity of the companion for different companion masses; in this case $\tau_e/\tau_a = 0.1$. The key refers to the mass of the companion in M_{Jup} and inner / outer denotes the initial position of the $10 M_{\text{Jup}}$ planet. The lines trace the evolution of the eccentricity from zero, terminating either at 10^6 yr, at the ejection of one of the planets or at a collision (between the two planets or with the star). The grey shaded area shows the 1σ interval of the observed eccentricity in CI Tau.

scale free is due to the finite size of the star and planets which allows us to distinguish close scattering events from physical collisions.

The results of this exercise are shown in Fig. 4 when only the eccentricity of the outer planet is damped. The densely filled region of orbital parameters at low eccentricity corresponds to when the

planets are exchanging eccentricity cyclically but where the eccentricities are sufficiently low to avoid close scattering events. The eccentricity of the massive planet never exceeds 0.1–0.2 during the former phase; therefore, if the eccentricity of the planet in CI Tau is as high as ~ 0.3 then this must have resulted from interactions in the latter regime. The scattering regime (typically lasting $\sim 10^3$ yr) is characterized by large stochastic excursions in the eccentricity plane which are terminated at the point that the planets collide, the lower mass planet is ejected from the system or the lower mass planet collides with the star (in the case that the massive planet is the interior one, these outcomes occur respectively ~ 5 per cent, 55 per cent, 40 per cent of the time in the 100 simulations we have run). Any of these outcomes would remove the light planet from the vicinity of the heavy planet. We therefore conclude that in any scenario in which a planet acquired significant eccentricity through pumping by a sibling planet, this sibling should not remain in its vicinity. In order to check the sensitivity to our calibration of the eccentricity damping time-scale, we have run models with $\tau_e/\tau_a = 0.01$ or 1 coming to the same conclusion – the eccentricity of the planet in CI Tau cannot have reached $e > 0.2$ through planet–planet interactions unless a strong scattering event occurs, and this typically removes the lighter planet from the system.

4 DISCUSSION AND CONCLUSION

So far we have considered various eccentricity driving mechanisms assuming these operate close to the planet’s present position. Given that it is unlikely that the planet formed at 0.1 au, we need also to consider scenarios for its inward migration from larger radius.

While there have been conflicting results as to whether the development of eccentricity inhibits disc mediated migration (Papaloizou et al. 2001; D’Angelo et al. 2006; Rice, Armitage & Hogg 2008; Duffell & Chiang 2015), there is some suggestion that eccentricity growth is favoured at low H/R (Armitage & Natarajan 2005). Since discs are generally flared (H/R increases with R), this would favour growth at small radii, possibly delaying the excitation of eccentricity until the planet arrives at its present location. Also, our own simulations, which are the only ones to have studied the migration of eccentric planets over such long time-scales, however find that eccentric planets can migrate (see Fig. 1) and in this case the eccentricity may be excited anywhere between its birthplace and current location. We find (in simulations for which e is as large

as 0.15) that the planet migrates at a rate that is consistent with the rate found in simulations involving planets on circular orbits [Duffell et al. (2014) and Dürmann & Kley (2015)]. The migration time can be approximated as $t_{\text{mig}} = t_v \max(1, \frac{M_p}{\Sigma \pi a^2})$, where t_v is the viscous time-scale.⁶ For the massive planet considered here, the second term in brackets is relevant within ~ 10 au (i.e. the planetary inertia is important) so that for a steady state disc we have $t_{\text{mig}} \sim 10M_p/\dot{M}$, independent of radius and viscosity assumptions. For the parameters of CI Tau, this implies $t_{\text{mig}} \sim 1$ Myr.

It is tempting to ascribe some significance to the fact that the radius of the observed planet is only ~ 30 per cent beyond the corotation radius between the star and the disc (assuming that the 7 d photometric period of the star measured by Johns-Krull et al. 2016 is the star's rotation period). Models of disc braking of young stars suggest that systems evolve to a state of disc locking where the disc is truncated slightly inside the corotation radius. A migrating planet is expected to stall as it enters the magnetospheric cavity (Romanova & Lovelace 2006; Papaloizou 2007) so that if another planet arrives at small radii through disc migration, a dynamical interaction between the two is assured at this location. In around 40 per cent of the cases studied in Section 3, the remaining 10 Jupiter mass planet is scattered outward in the interaction while the lighter sibling planet ends up being swallowed by the star. This provides a plausible explanation for why the planet is located in the vicinity of, but not exactly at, the expected radius of the magnetospheric cavity.

Alternatively, if disc mediated migration is effective at moderate eccentricity, then the dynamical interaction can have occurred at a range of radii. While the subsequent migration may be accompanied by a damping of the eccentricity to the equilibrium value excited by the disc, this would take $\sim 10^6$ yr (longer if τ_e is larger at large e , as found by Papaloizou & Larwood 2000). In this case, the proximity of the observed planet to the putative magnetospheric cavity is coincidental and the planet is likely still migrating.

ACKNOWLEDGEMENTS

We thank J. Papaloizou, L. Prato, and E. Ragusa for interesting discussions and the referee for improving the clarity of the paper. This work has been supported by the DISCSIM project, grant agreement 341137 funded by the European Research Council under ERC-2013-ADG, and from STFC through grant ST/L000636/1. This work used the DIRAC Shared Memory Processing and Data Analytic systems, both at the University of Cambridge and operated, respectively, by the COSMOS Project at the Department of Applied Mathematics and Theoretical Physics and the Cambridge High Performance Computing Service, on behalf of the STFC DiRAC HPC Facility (www.dirac.ac.uk). This equipment was funded by BIS National E-infrastructure capital grants ST/J005673/1 and ST/K001590/1, STFC capital grants ST/H008586/1, ST/H008861/1 and ST/H00887X/1, STFC DiRAC Operations grant ST/K00333X/1, and STFC DiRAC Operations grant ST/K00333X/1. DiRAC is part of the National E-Infrastructure.

REFERENCES

Andrews S. M., Williams J. P., 2007, *ApJ*, 659, 705
Armitage P. J., Natarajan P., 2005, *ApJ*, 634, 921

⁶ The formula ignores the recent findings that type II migration is a factor of 2–3 faster than the viscous time-scale as the ones presented here are order-of-magnitude estimates, but it does catch the correct dependence with the disc mass.

- Barker A. J., Ogilvie G. I., 2009, *MNRAS*, 395, 2268
Benítez-Llambay P., Ramos X. S., Beaugé C., Masset F. S., 2016, *ApJ*, 826, 13
Bitsch B., Crida A., Libert A.-S., Lega E., 2013, *A&A*, 555, A124
Chambers J. E., 1999, *MNRAS*, 304, 793
Chauvin G., Lagrange A.-M., Dumas C., Zuckerman B., Mouillet D., Song I., Beuzit J.-L., Lowrance P., 2004, *A&A*, 425, L29
Chauvin G., Lagrange A.-M., Dumas C., Zuckerman B., Mouillet D., Song I., Beuzit J.-L., Lowrance P., 2005, *A&A*, 438, L25
Chiang E., Laughlin G., 2013, *MNRAS*, 431, 3444
Ciardi D. R. et al., 2015, *ApJ*, 809, 42
Cresswell P., Dirksen G., Kley W., Nelson R. P., 2007, *A&A*, 473, 329
D'Angelo G., Lubow S. H., Bate M. R., 2006, *ApJ*, 652, 1698
David T. et al., 2016, *Nature*, 534, 658
Donati J. et al., 2016, *Nature*, 534, 662
Duffell P. C., Chiang E., 2015, *ApJ*, 812, 94
Duffell P. C., Haiman Z., MacFadyen A. I., D'Orazio D. J., Farris B. D., 2014, *ApJ*, 792, L10
Dunhill A. C., Alexander R. D., Armitage P. J., 2013, *MNRAS*, 428, 3072
Dürmann C., Kley W., 2015, *A&A*, 574, A52
Flock M., Fromang S., González M., Commerçon B., 2013, *A&A*, 560, A43
Goldreich P., Sari R., 2003, *ApJ*, 585, 1024
Goldreich P., Tremaine S., 1980, *ApJ*, 241, 425
Guilloteau S., Dutrey A., Piétu V., Boehler Y., 2011, *A&A*, 529, A105
Guilloteau S., Simon M., Piétu V., Di Folco E., Dutrey A., Prato L., Chapillon E., 2014, *A&A*, 567, A117
Hansen B. M. S., Murray N., 2013, *ApJ*, 775, 53
Johns-Krull C. M. et al., 2016, *ApJ*, 826, 206
Kraus A. L., Ireland M. J., 2012, *ApJ*, 745, 5
Lee M. H., Peale S. J., 2002, *ApJ*, 567, 596
Lega E., Morbidelli A., Nesvorný D., 2013, *MNRAS*, 431, 3494
Lin D. N. C., Bodenheimer P., Richardson D. C., 1996, *Nature*, 380, 606
Lubow S. H., 1991a, *ApJ*, 381, 259
Lubow S. H., 1991b, *ApJ*, 381, 268
McClure M. K. et al., 2013, *ApJ*, 775, 114
Marois C., Macintosh B., Barman T., Zuckerman B., Song I., Patience J., Lafrenière D., Doyon R., 2008, *Science*, 322, 1348
Marzari F., Baruteau C., Scholl H., 2010, *A&A*, 514, L4
Moeckel N., Armitage P. J., 2012, *MNRAS*, 419, 366
Murray C. D., Dermott S. F., 2000, *Solar System Dynamics*. Cambridge Univ. Press, Cambridge
Neuhäuser R., Guenther E. W., Wuchterl G., Mugrauer M., Bedalov A., Hauschildt P. H., 2005, *A&A*, 435, L13
Neuhäuser R., Mugrauer M., Seifahrt A., Schmidt T. O. B., Vogt N., 2008, *A&A*, 484, 281
Papaloizou J. C. B., 2007, *A&A*, 463, 775
Papaloizou J. C. B., Larwood J. D., 2000, *MNRAS*, 315, 823
Papaloizou J. C. B., Nelson R. P., Masset F., 2001, *A&A*, 366, 263
Rasio F. A., Ford E. B., 1996, *Science*, 274, 954
Rice W. K. M., Armitage P. J., Hogg D. F., 2008, *MNRAS*, 384, 1242
Romanova M. M., Lovelace R. V. E., 2006, *ApJ*, 645, L73
Sallum S. et al., 2015, *Nature*, 527, 342
Shakura N. I., Sunyaev R. A., 1973, *A&A*, 24, 337
Stauffer J. et al., 2014, *AJ*, 147, 83
Suzuki T. K., Muto T., Inutsuka S.-I., 2010, *ApJ*, 718, 1289
Tanaka H., Ward W. R., 2004, *ApJ*, 602, 388
Teyssandier J., Ogilvie G. I., 2016, *MNRAS*, 458, 3221
Teyssandier J., Terquem C., 2014, *MNRAS*, 443, 568
van Eyken J. C. et al., 2012, *ApJ*, 755, 42
Xiao H. Y., Covey K. R., Rebull L., Charbonneau D., Mandushev G., O'Donovan F., Slesnick C., Lloyd J. P., 2012, *ApJS*, 202, 7

This paper has been typeset from a $\text{\TeX}/\text{\LaTeX}$ file prepared by the author.